oxide (ITO) as a potential transparent conducting material. In addition, CPPy nanoparticles could be applied as an anodic material in lithium-ion batteries because of their high conductivity and large surface area.

We have demonstrated a surfactant-mediated methodology for the synthesis of 2 nm spherical PPy nanoparticles. The carbonized PPy nanoparticles can be used as a highly transparent conductive material, which may possibly be a substitute for carbon nanofibers. Importantly, low-temperature microemulsion polymerization may provide a facile way to synthesize new polymer nanoparticles, and might be expanded to allow the fabrication of ultrafine metallic and inorganic particles, which embraces the concept of "nanoreactors".

Experimental Section

A variable amount of surfactant was magnetically stirred in distilled water (40 mL) at 3 °C. Pyrrole monomer (1.0 g, 14.9 mmol) was added dropwise to the surfactant solution, and iron(III) chloride hexahydrate (9.25 g, 34.3 mmol), dissolved in distilled water (5 mL), was added to the surfactant/pyrrole solution. Microemulsion polymerization proceeded while stirring for 3 h at 3 °C. The reaction product was placed in a separating funnel and excess methanol was added to remove the surfactants and the residual iron(III) chloride. The upper layer was discarded and the remaining nanoparticle precipitate was dried in a vacuum oven at room temperature.

The PPy nanoparticles were placed in a quartz tube in a furnace under N_2 atmosphere. The sample was heated to 800 °C at a heating rate of 3 °C min^{-1}, held at 800 °C for 5 h, and then cooled to room temperature.

PPy nanoparticles and PC were combined in THF. The mixed solution was spin-coated onto a glass slide using a PWM32 spinner (Headway Research, Inc.). Transparency of the films was measured with a UV/Vis spectrometer and the conductivity was determined by the van der Pauw method. As-prepared (AP)-grade CNs were purchased from Aldrich. PC/CN and PC/CPPy films were prepared by the same method. Film thicknesses were estimated with an Alpha-Step 500 surface profiler (Tencor). All films were approximately 270 nm thick, the growth being controlled by changing the spinning speed. TEM images were taken by a JEOL 2010 high-resolution microscope and EDAX analysis was carried out using a Philips CM 20 microscope.

Received: March 26, 2002
Revised: August 26, 2002 [Z18986]

[1] a) A. J. Zarur, J. Y. Ying, *Nature* **2000**, *403*, 65 – 67; b) A. K. Boal, F. Ilhan, J. D. Derouchey, T. Thurn-Albrecht, T. P. Russell, V. M. Rotello, *Nature* **2000**, *404*, 746 – 748; c) V. F. Puntes, K. M. Krishnan, A. P. Alivisatos, *Science* **2001**, *291*, 2115 – 2117.
[2] a) F. Caruso, R. A. Caruso, H. Möhwald, *Science* **1998**, *282*, 1111 – 1114; b) Y. Lu, H. Fan, A. Stump, T. L. Ward, T. Rieker, C. J. Brinker, *Nature* **1999**, *398*, 223 – 226.
[3] a) S. A. Johnson, P. J. Ollivier, T. E. Mallouk, *Science* **1999**, *283*, 963 – 965; b) G. Zhang, A. Niu, S. Peng, M. Jiang, Y. Tu, M. Li, C. Wu, *Acc. Chem. Res.* **2001**, *34*, 249 – 256.
[4] a) F. Reynolds, K. Jun, Y. Li, *Macromolecules* **2001**, *34*, 167 – 170; b) X. J. Xu, K. S. Siow, M. K. Wong, L. M. Gan, *Langmuir* **2001**, *17*, 4519 – 4524.
[5] S. Zhou, F. Yeh, C. Burger, B. Chu, *J. Phys. Chem. B* **1999**, *103*, 2107 – 2112.
[6] W. Meier, *Curr. Opin. Colloid Interface Sci.* **1999**, *4*, 6 – 14.
[7] J. Jang, K. Lee, *Chem. Commun.* **2002**, *10*, 1098 – 1099.
[8] H. Oka, M. Inagaki, Y. Kaburagi, Y. Hishiyama, *Solid State Ionics* **1999**, *121*, 157 – 163.
[9] E. Ando, S. Onodera, M. Iino, O. Ito, *Carbon* **2001**, *39*, 101 – 108.
[10] M. Inagaki, K. Fujita, Y. Takeuchi, K. Oshida, H. Iwata, H. Konno, *Carbon* **2001**, *39*, 921 – 929.
[11] F. Yan, G. Xue, M. Zhou, *J. Appl. Polym. Sci.* **2000**, *77*, 135 – 140.
[12] D. Shibuta, US Patent 5,853,877 **1996**.

Novel Capsules with High Stability and Controlled Permeability by Hierarchic Templating**

Zhifei Dai, Lars Dähne,* Helmuth Möhwald, and Brigitte Tiersch

Hollow capsules with high stability and controllable permeability have very interesting actual and potential applications, for example, as constrained environments for the preparation of nanostructured materials, the encapsulation of guest molecules, drug delivery, catalysis, and as host containers for nucleic acid storage and transport.[1,2] However, deformation and rupture of hollow capsules under shear stress may limit these applications. The stability can be increased slightly by deposition of additional layers, but the permeability decreases simultaneously. While the loading has to be fast and the release slow in most applications, the permeability of the capsules has to be tuned according to the specific application.[3] Therefore, it is desirable to develop a simple and reliable method to fabricate capsules with high stability and the desired permeability. A combination of tailorable and tunable silica nanoparticles with layer-by-layer (LbL) self-assembly[4] provides a powerful tool for the creation of exciting nanostructured systems. Silica is extremely well-suited to this purpose since well-defined particles can be prepared. Since silica is itself charged, it can be assembled with cationic polyelectrolytes, and the chemistry to dissolve it without affecting the chemical composition of the organic film components is already well established.

Here we make use of these features to prepare capsule walls of defined porosity after removal of SiO_2 (Figure 1, left) or sphere-in-sphere (SiS) structures, again after removal of SiO_2, that is sandwiched in high concentration between two indestructible walls (Figure 1, right). Similar structures can be found in nature, for example, gram-negative bacteria possess two cell walls which are separated by an aqueous phase.[5] To prepare nanoporous shells (NPS) we have used SiO_2 covered by polyallylamine hydrochloride (PAH@silica) as the cationic polyelectrolyte and polystyrene sulfonic acid (PSS) as the anionic polyelectrolyte and deposited multilayers of these by consecutive alternating adsorption on melamine formaldehyde particles (MF). The MF core is then removed by treatment with HCl, and the SiO_2 dissolved with HF. To form SiS shells, multilayers of PSS and PAH (2–3 double layers) are adsorbed alternately, followed by a variable number of silica and PAH layers (1–3 double layers) and then PSS and PAH to build-up a nondestuctable outer shell.

[*] Dr. L. Dähne, Dr. Z. Dai, Prof. H. Möhwald
Max-Planck Institute of Colloids and Interfaces
14476 Golm (Germany)
Fax: (+ 49) 30-6392-3601
E-mail: lars.daehne@capsulution.com
Dr. B. Tiersch
Department of Colloid Chemistry
Institute of Physical and Theoretical Chemistry
University of Potsdam, 14476 Golm (Germany)

[**] The authors are grateful to H. Zastrow for providing 50-nm silica particles. This work was supported by BMBF and BASF.

  0044-8249/02/4121-4019 $ 20.00+.50/0

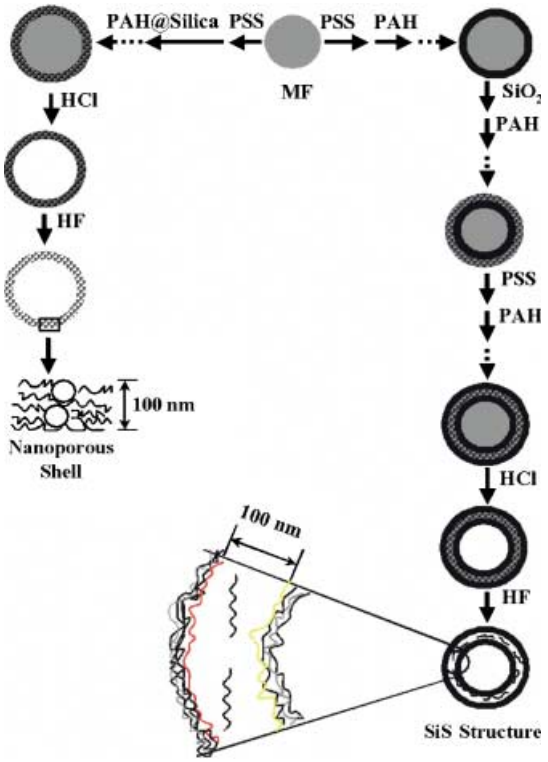

Figure 1. General procedure for the preparation of hollow capsules possessing nanopores and sphere-in-sphere shells.

To distinguish the inner and outer shells by optical spectroscopy we partly coadsorb PAH labeled with fluorescein isothiocyanate (PAH-FITC, green fluorescence) to the inner shell and PAH labeled with rhodamine B (PAH-RhB, red fluorescence) to the outer shell. Removal of the MF core by treatment with HCl again yields a hollow capsule. Subsequent removal of the SiO_2 by HF yields a liquid interlayer in which excess PAH is dissolved. This space between the outside volume and inner core volume is itself interesting as a reaction space, but here we use it merely to tune the properties of the capsule wall as a whole.

The wall thickness of both NPS and SiS capsules was measured by means of scanning-force microscopy (SFM) and shows there is a large difference in the capsules in the dried state before and after removal of the silica particles. A typical SFM image is shown in Figure 2. NPS capsules of (PSS/PAH@silica)$_4$ have average diameters of about 6.0 and 4.3 μm. The wall thickness of the dried particles can be deduced from SFM contour plots, since, for example, the height terraces correspond to folds and thus to a double wall thickness or multiples

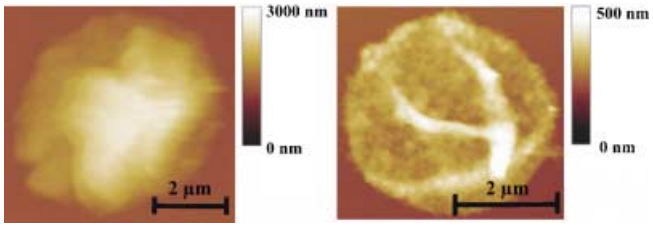

Figure 2. SFM images of air-dried hollow capsules of (PSS/PAH@silica)$_4$: a) before and b) after removal of silica nanoparticles from inside the walls.

thereof. In this case, one derives a value of 18 nm and, less accurately, of 500 nm for the wall thickness after and before removal of the SiO_2, respectively. An average diameter increment of approximately 120 nm per PAH@silica multilayer indicates that about two monolayers (on average) of silica nanoparticles are adsorbed with each deposition cycle. This may be a result of the formation of agglomerates of silica nanoparticles. Nevertheless, SiS capsules of (PSS/PAH/PSS/PAH-FITC)(silica/PAH/silica)(PAH-RhB/PSS/PAH/PSS/PAH) possess a capsule wall containing silica particles with a thickness of 120–126 nm. The removal of the silica layers left a wall thickness of approximately 20–26 nm. The difference of about 100 nm corresponds to the thickness of two silica layers. Thus, SFM measurements indicate silica nanoparticles were successfully incorporated into the wall of the capsules and removed by HF etching.

NPS capsules were resolved by ultramicrotom transmission electron microscopy (UM-TEM). It can be seen from UM-TEM images (Figure 3) that the resulting hollow capsules of

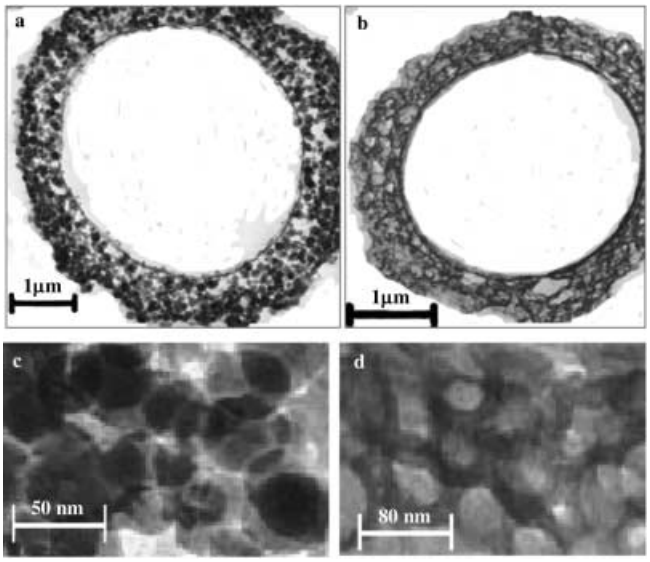

Figure 3. UM-TEM images of capsules of (PSS/PAH@silica)$_4$: before (a, c) and after (b, d) removal of silica particles from inside the walls.

(PSS/PAH@silica)$_4$ are almost spherical. Capsules with silica particles (dark dots with brighter surrounding) are shown in Figure 3a. After the capsules have been subjected to HF acid to remove silica particles, the resulting pores (bright area with darker surrounding) are randomly distributed over the thin polymer shell of about 500 nm thickness, whereas the center with a diameter of about 4 μm is totally empty (Figure 3b). The pore size distribution depends on the size of the silica particles and the osmotic pressure in the pores, and results in the thickness of the porous shell being similar to that of the shell possessing silica particles. The much smaller thickness measured by SFM after SiO_2 removal is thus the result of a collapse of the pores upon drying. Figure 3c and d show the silica particles and the resulting nanopores at higher resolution.

It can be seen by means of confocal laser scanning microscopy (CLSM) that both the NPS and SiS capsules are

  0044-8249/02/4121-4020 $ 20.00+.50/0

shape-persistent, with no agglomeration in solution before or after removal of the silica particles. More insight into the structure of the SiS shells in liquid has been obtained by high-resolution confocal two-color fluorescence microscopy. Removal of the silica layers should form an interlayer of approximately 100 nm thickness in between the inner shell of (PSS/PAH/PSS/PAH-FITC; approximately 8 nm thickness) and the outer shell of (PAH-RhB/PSS/PAH/PSS/PAH); approximately 10 nm thickness) that is filled by a PAH solution. Figure 4a shows the occurrence of two completely

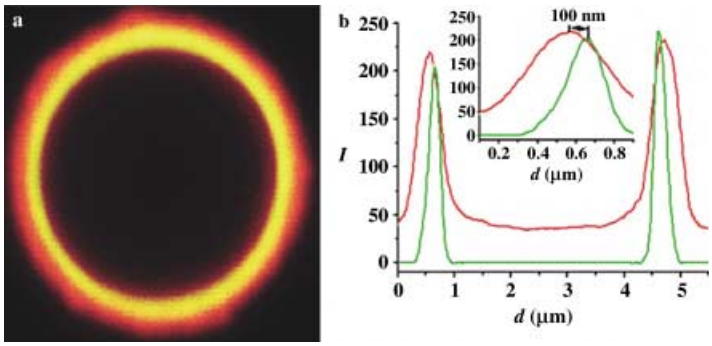

Figure 4. a) CLSM fluorescence image of a capsule of (PSS/PAH/PSS/PAH-FITC)(silica/PAH/silica)(PAH-RhB/PSS/PAH/PSS/PAH) after removal of the silica layers. Red emission results from the rhodamine B in the outer layers and yellow emission from the fluorescein in the inner layers mixed with the emission from the rhodamine B. b) Fluorescence profiles along a line through the capsule center; green: fluorescein fluorescence, red: rhodamine B fluorescence. I = fluorescence intensity.

co-centered fluorescent shells, which are attributed to the fluorescein-labeled inner shell of PSS/PAH/PSS/PAH-FITC and the rhodamine B labeled outer shell of PAH-RhB/PSS/PAH/PSS/PAH. Figure 4b show the fluorescence distribution of both dyes detected simultaneously at different wavelengths. The insert of Figure 4b shows the distance between the inner and the outer shells at higher resolution. The difference between both maxima taken from five profiles yields an average distance of 100 ± 10 nm between the PAH-FITC on the inner shell and the PAH-RhB on the outer shell. This distance agrees well with the value of 100 nm determined by SFM for the silica-layer thickness.

The permeability was studied by confocal microscopy studies on the fluorescently labeled PAH and PSS, as well as on small dye molecules such as fluorescein and rhodamine B. NPS capsules are impermeable to the polymer but permeable to small dye molecules, both before and after removal of the silica particles. No difference in permeability was observed for SiS capsules before and after removal of the silica layers. However, annealing the SiS capsules with silica interlayers in the walls at 70 °C for 6 min and then cooling them down results in them becoming impermeable to small dye molecules, similar to the $(PSS/PAH)_5$ capsules. On the other hand, SiS capsules obtained by removal of the silica interlayers are permeable to small molecular dyes and impermeable to polymers.

The reduced permeability of the $(PSS/PAH)_5$ and $(PSS/PAH)_2$(silica/PAH/silica)$(PAH/PSS)_2$/PAH capsules was ascribed to a rearrangement of the macromolecular layer constituents after annealing.[6] This situation arises from a stronger coupling of the polyelectrolytes with each other which leads to an increased network in the wall. Macroscopically, the rearrangement reduces the capsule diameter by more than 20 %. Simultaneously, the capsule wall contracts so that even small molecules cannot permeate through. Although the overall wall material of the SiS capsules after removal of silica is almost the same as for the $(PSS/PAH)_6$ capsules, the original continuous shell is divided into two subshells by the liquid interlayer. Thus, it is understandable that small dye molecules diffuse more easily into SiS capsules with a liquid interlayer than into $(PSS/PAH)_6$ capsules.

The mechanical stability of the capsules was elucidated by observing osmotically induced deformations. PSS (M_W = 70000 Da) does not permeate the capsule wall, hence, the capsule morphology can be tuned by adjusting the osmotic pressure external to the PSS solution. Starting with perfectly spherical capsules, a stepwise increase in concentration of PSS osmotically leads to permeation of water from the inside to the outside and concomitant deformation of the capsules. If $(PSS/PAH)_5$ and $(PSS/PAH)_6$ capsules are incubated in a 12 % PSS solution, they invaginate and no longer show a spherical shape.[6] However, no deformation was observed for either the NPS and SiS capsules before or after removal of the silica.

It can be easily understood that rigid organic–inorganic capsules are deformation-resistant, even under a considerable mechanical stress. After removal of the silica particles, capsules with water interlayers or nanopores have the same chemical composition as the capsules obtained from PSS/PAH. The much higher mechanical stability, which is attributed to the different shell structure, may arise from two factors: either the wall has become reinforced by the silica removal process (for example, by incomplete removal of silica or cross-linking of some chains) or the excess PAH resulting from the removal of silica particles has been excreted from the wall into the water interlayer or nanopores and build up an osmotic pressure. The latter offsets the external osmotic pressure of 10^6 N m^{-2} corresponding to a weight of 12 % PSS. The intermediate water layer must also exhibit a similar polyelectrolyte concentration. Such a concentration is not unreasonable because the PAH content in the silica-containing interlayer can be estimated to be about 11 %. This estimate results from assuming a silica particle has a diameter of 50 nm and the polyelectrolyte coating has a thickness of 2 nm.

In summary, our results have shown that intriguing capsules with vastly different mechanical stability and controllable permeability can be prepared simply by changing the structure of the shell. We expect these novel capsules to be of particular interest for applications, such as delivery systems, catalysis, and chemical sensing or separation, for which structural features such as selective permeability, cavity shape, as well as a remarkable mechanical stability are critical. It is also clear that the liquid interlayer between the polymeric walls may be a reaction compartment suitable for reactions to enable the wall properties to be changed further. Further experiments need to be carried out to increase the efficiency and sophistication of encapsulation, delivery, and separations with these capsules.

  0044-8249/02/4121-4021 $ 20.00+.50/0

Experimental Section

PSS ($M_W = 70000$ Da) and PAH ($M_W = 70000$ and 15000 Da) were obtained from Aldrich. Silica particles (50 nm) were prepared according to the method reported by Stöber et al.[7] MF particles (3.99 μm) were purchased from Microparticles GmbH, Germany.

The procedure employed for the deposition of PSS, PAH, silica, and PAH-coated silica nanoparticles onto the surface of MF microparticles is as follows: A solution (1.5 mL) of the species with a charge opposite to that of the MF templates or the last layer deposited (1 mg mL^{-1} PSS or PAH in 0.5 M NaCl or 2 wt% silica or PAH-coated silica nanoparticles in 0.1 N NaCl) was added to a template latex solution (0.3 mL) and left to adsorb for 15 min. The excess added species was removed after each layer was deposited by centrifugation (2000 g, 2 min)/washing/redispersion cycles (× 3) with dilute aqueous NaCl. After the final washing step, the particles were redispersed in water (0.3 mL). Subsequent layers were deposited until the desired number of multilayers was achieved. Silica particles (50 nm) were covered with one PAH layer by using a similar procedure except that centrifugation (10000 rpm, 10 min) was used for the particle separation. Hollow capsules were prepared by dissolving the MF cores with 0.1 M HCl solution. Silica particles in the walls of the capsules were removed with 0.1 M HF solution.

Confocal micrographs were taken with a confocal laser scanning microscope "Aristoplan" from Leica (Germany) equipped with a 100 × oil immersion objective.

The morphology of the capsule wall was investigated by transmission electron microscopy of ultrathin sections. The sections were made on an ultramicrotom "Ultracut E" after embedding them in a mixture of methyl methacrylate and *n*-butyl methacrylate. The sections were observed through a Zeiss EM 902 transmission electron microscope.

Received: April 5, 2002
Revised: July 15, 2002 [Z19050]

[1] a) E. Donath, G. B. Sukhorukov, F. Caruso, S. A. Davis, H. Möhwald, *Angew. Chem.* **1998**, *110*, 2324 – 2327; *Angew. Chem. Int. Ed.* **1998**, *37*, 2202 – 2205; b) F. Caruso, R. Caruso, H. Möhwald, *Science* **1998**, *282*, 1111 – 1113.

[2] a) Z. F. Dai, A. Voigt, S. Leporatti, E. Donath, L. Dähne, H. Möhwald, *Adv. Mater.* **2001**, *13*, 1339 – 1342; b) G. Sukhorukov, L. Dähne, J. Hartmann, E. Donath, H. Möhwald, *Adv. Mater.* **2000**, *12*, 112 – 115; c) Z. F. Dai, L. Dähne, E. Donath, H. Möhwald, *Langmuir* **2002**, *18*, 4553 – 4555.

[3] a) K. Park, *Controlled Drug Delivery: Challenges and Strategies*, American Chemical Society, Washington, DC, **1997**; b) R. Langer, *Nature* **1998**, *392*, 5 – 10; c) A. J. Ribeiro, R. J. Neufeld, P. Arnaud, J. C. Chaumeil, *Int. J. Pharm.* **1999**, *187*, 115 – 123.

[4] G. Decher, Science **1997**, *277*, 1232 – 1237.

[5] a) T. Schirmer, T. A. Keller, Y. F. Wang, J. P. Rosenbusch, *Science* **1995**, *267*, 512 – 514; b) M. Winterhalter, C. Hilty, S. M. Bezrukov, C. Nardin, W. Meier, D. Fournier, *Talanta* **2001**, *55*, 965 – 971.

[6] a) C. Y. Gao, E. Donath, S. Moya, V. Dudnik, H. Möhwald, *Eur. Phys. J. E* **2001**, *5*, 21 – 27; b) S. Leporatti, C. Gao, A. Voigt, E. Donath, H. Mohwald, *Eur. Phys. J. E* **2001**, *5*,13 – 20.

[7] W. Stöber, A. Fink, E. Bohn, *J. Colloid Interface Sci.* **1968**, *26*, 62 – 69.

Ru^{II} Complexes of "Large-Surface" Ligands**

Edith C. Glazer and Yitzhak Tor*

Ru^{II}–polypyridyl complexes have traditionally been synthesized by a complexation reaction of the ligand of interest with the appropriate Ru^{II} precursors.[1] Although significant advances have been made in synthesizing modified 2,2′-bipyridine-, 1,10-phenanathroline-, and 2,2′:6,2″-terpyridine-type ligands, these methodologies provide access to a rather constrained set of structural motifs.[2] In particular, the range of Ru^{II} complexes that contain large, extended surfaces is limited,[3] despite their enormous potential as nucleic acid intercalators, luminescent probes, as well as energy and electron donors and acceptors.[4,5] We envisage a new methodology for the fabrication of extended polypyridyl systems from modular building blocks by the dehydrogenation reaction of a strained metal-complexed ligand (Scheme 1).[6,7]

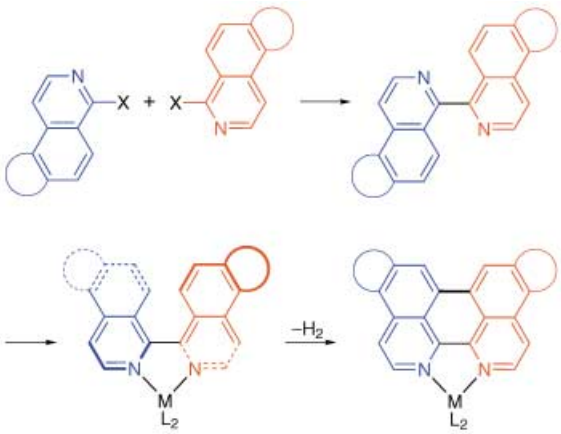

Scheme 1. Extended symmetric and asymmetric bipyridine-type ligands are synthesized in a modular fashion from simpler heterocycles. The chelating ligand is enforced into a *syn* orientation within an octahedral complex and can then undergo a dehydrogenation reaction to a planar "large-surface" metal–polypyridine complex.

In this modular approach, nitrogen-containing heterocycles are homo- or heterocoupled to give extended bipyridines that can subsequently be coordinated and dehydrogenated to give the desired coordination complexes (Scheme 1).[8] Here we report the successful implementation of this strategy for the preparation of biologically active eilatin-containing complexes as well as Ru^{II} complexes of previously unknown "large-surface" ligands.

[*] Prof. Dr. Y. Tor, E. C. Glazer
Department of Chemistry and Biochemistry
University of California, San Diego
La Jolla, CA 92093-0358 (USA)
Fax: (+1) 858-534-0202
E-mail: ytor@ucsd.edu

[**] We thank the National Institutes of Health (Grant No. GM 58447) for generous support. We are grateful to Dr. Moshe Kol for authentic samples of eilatin-containing complexes.

Supporting information for this article is available on the WWW under http://www.angewandte.org or from the author.

  0044-8249/02/4121-4022 $ 20.00+.50/0